Center for Turbulence Research
Proceedings of the Summer Program 1994

Instability of streamwise vortices in plane channel flows

By K. Coughlin[1], J. Jiménez[2] AND R. D. Moser[3]

We present analysis and numerical experiments on the instability of streamwise vortices in 'minimal channel' flows and argue that this instability is a key feature in the observed intermittent cycle of formation, break-up, and re-formation of these structures. The base flow is a three-component, two-dimensional pair of counter-rotating rolls with axes aligned along the direction of the mean shear. While it is not a steady solution to the Navier-Stokes equations, we show numerically that this flow is unstable on a fast time scale to a secondary, three-dimensional Floquet mode. The growth of the secondary instability does not saturate in a new equilibrium, but continues until highly unstable local shear layers form and the entire flow breaks down into turbulence. Our analysis is motivated in part by the strong similarities between the intermittent turbulent cycle in minimal channel flows and one studied, both experimentally and in computations, in Couette-Taylor flow.

1. Introduction

The existence of coherent structures in boundary layers has a significant effect on the dynamics of wall-bounded turbulence, and a great deal of work has been done to try to characterize and explain their dynamics. The structures have been identified as streamwise 'streaks' of relatively low speed fluid and are associated with the existence of pairs of counter-rotating, streamwise vortices. Dynamically, the streaks are created as part of a repeating cycle of formation, break-down, and regeneration. While the specific mechanisms of streak formation vary from case to case, certain characteristics of the break-down process appear to be quite general. In particular, the streaks are typically observed to become wavy with the waviness increasing until the coherence of the flow breaks down into turbulence.

A number of investigators have looked in more detail at the process of streak break-down in different situations. Swearingen & Blackwelder (1987), using Görtler vortices as an experimental model of the coherent structures in planar geometries, found that the resulting streaks were unstable to downstream traveling waves, and subsequently to a rapid breakdown into turbulence.

The instability was attributed to the spanwise velocity gradient created by the streamwise vortex/streak combination. Jiménez & Moin (1991), in numerical computations of plane Poiseuille flow in a doubly periodic channel, found that turbulence could be sustained provided that the the spanwise dimension was larger than

1 CERCA, University of Montreal, Canada
2 Center for Turbulence Research
3 NASA Ames Research Center

about 100 wall units. In these so-called 'minimal channels', the flow consists of a single low-velocity streak, which undergoes an intermittent cycle of onset and collapse of turbulence. The onset of turbulence is again associated with the appearance and growth of a sinusoidal perturbation of the streak. Hamilton *et al.* (1994), in minimal channel calculations of plane Couette flow, found the same type of intermittent, turbulent cycle and further evidence that breakdown of the streaks is associated with some kind of instability mechanism.

Recently, an intermittent turbulent cycle similar to those occurring in minimal channels was discovered experimentally in Couette-Taylor flow (Hammil *et al.*, 1994). In this system, fluid is confined between parallel, concentric cylinders which rotate independently. It can be thought of as a parallel shear layer with experimentally realizable, periodic boundary conditions in the streamwise direction. Using direct numerical simulations, Coughlin & Marcus (1994) have formulated a simple conceptual model which accounts for most of the observed features of the flow. The feature most relevant to this paper is that the onset of turbulence is directly attributable to a well-defined linear instability of coherent structures (Taylor vortices) in the flow. This supports the idea that there is some generic mechanism whereby streamwise vortical structures in a parallel shear become unstable, and their instability leads to the onset of turbulence.

The purpose of this paper is to investigate this idea further, making use of analogies with the Couette-Taylor system. In the latter, careful analysis of transient data and subsequent design of appropriate numerical experiments were used to verify that a linear mechanism was involved in the transition process. Briefly, coherent structures (spiral Taylor vortices) form in the Couette-Taylor system due to centrifugal instability, and then go unstable to secondary modes (modulated traveling waves). The spatial configuration of the secondary mode is such that, when it grows linearly to large enough amplitude, strong local shear layers are produced, and these trigger the sudden onset of the turbulence. The turbulence has a finite lifetime simply because energy is dissipated by turbulent fluctuations at a faster rate than the mean flow can draw energy through the torques at the walls. After the turbulence collapses, the coherent structures reform, and the cycle repeats (Coughlin & Marcus, 1994).

We hypothesize that essentially the same type of cycle is occurring in plane channel flows (we consider only the minimal channel, for which the cycle is roughly periodic in time). The analysis relies on treating the streamwise rolls/streaks as a quasi-equilibrium, and investigating their stability. We find that the rolls are indeed unstable to a secondary, three-dimensional mode, which can be characterized by its symmetry and time dependence. This mode grows linearly and, as in the Couette-Taylor system, its growth to large amplitude produces highly unstable local shear layers; hence, the transition to turbulence. The turbulence has a finite lifetime, the flow returns to its laminar configuration, and the cycle repeats. The intermittency in this cycle thus corresponds to quasi-regular excursions away from a flow configuration defined by the coherent structures plus the secondary mode.

In this paper, our focus is on the mathematical description of the instability for

several reasons. First, because it facilitates analysis of the physical mechanisms of instability. Second, because it is a necessary condition for modeling of the system: In our scenario, up to the onset of turbulence the flow is low-dimensional and, therefore, in principle can be modeled accurately using a small number of modes. From center manifold theory, we know that these modes must be the linear eigenmodes of the system and their nonlinear harmonics. The use of the right modes is essential to constructing models which can be useful in applications; if the modes chosen do not correspond to the real instabilities, there will be no reliable relation between the model parameters and the physical control parameters. Third, the state that the flow returns to during the laminar phase of each cycle, whether it is an equilibrium or not, is clearly an important starting point for trying to understand the more complex transition from order to turbulence. Flow visualizations verify that this state is the configuration characteristic of the coherent structures and their secondary instability mode.

The organization of the paper is as follows: In Section 2 we present a description of the conceptual model we propose for the intermittent turbulent cycle. We then give, in Section 3, a complete description of the symmetries in the problem, which have been used to verify some hypotheses of the model. Section 4 contains a presentation of the numerical results supporting the model, and Section 5 the conclusions and an outline of future work.

2. The conceptual model

2.1 Mathematical preliminaries

2.1.1 Definition of the channel

The base flow is assumed to be either plane Poiseuille (driven by a mean pressure gradient) or plane Couette (driven by motion of the walls). The channel half-width is h, and the velocity maximum (the centerline velocity for Poiseuille flow and the wall velocity for Couette flow) is U. The Reynolds number is Uh/ν, and we use U as the unit of velocity, h as the unit of length, and h/U as the unit of time. The velocities u, v, and w are the dimensionless streamwise (x), cross-stream (y), and spanwise (z) components respectively. In dimensionless units $x \in [0, l_x]$, $y \in [-1, 1]$, $z \in [0, l_z]$. The streamwise and spanwise wavenumbers are $\alpha = 2\pi/l_x$ and $\beta = 2\pi/l_z$. For plane Couette flow, the two-dimensional, steady, streamwise flow is $U(y) = y$ and the corresponding spanwise vorticity is $\Omega = -dU/dy = -1$. For Poiseuille flow, $U(y) = 1 - y^2$ and $\Omega = 2y$. Note that these flows differ in several important ways: First, the symmetry of the base flow under reflection in y is different, leading to different allowed symmetries for the two- and three-dimensional flows; second, in Poiseuille flow the non-uniformity of Ω across the channel distinguishes the wall and outer regions, whereas no such distinction exists for plane Couette flow; third, in Poiseuille flow there is always a positive net mass flux in the down-stream direction.

2.1.2 Numerical method

The Navier-Stokes equations are solved in a doubly periodic channel geometry using a spectral initial value code. The numerical computations were begun using

the code developed at CTR (Kim *et al.*, 1987), and continued using a similar code developed independently (Coughlin, 1994). The velocity field is represented as a Fourier-Tchebyshev sum:

$$\mathbf{u} = \sum_{m=-M/2+1}^{M/2} \sum_{k=-K/2+1}^{K/2} \mathbf{u}_{km}(y,t) e^{ik\alpha x} e^{im\beta z}, \tag{1}$$

with $\mathbf{u}_{km}(y,t) = \sum_{n=0}^{N} \mathbf{a}_{nkm}(t) T_n(y)$. We write $\mathbf{u}$ for the velocity component in physical space, and $\mathbf{u}_{km}$ for the same component in Fourier space. Since $\mathbf{u}$ is real, $\mathbf{u}_{km} = \bar{\mathbf{u}}_{-k-m}$, where the overbar denotes complex conjugation. No-slip boundary conditions are imposed at the walls, and the pressure boundary condition is chosen to enforce constant mass flux in the streamwise direction.

2.2 Formation of streamwise rolls

Curvature in the Couette-Taylor system is responsible for the initial appearance of the Taylor vortices, and this constitutes the biggest difference from planar channels. In the latter, there is as yet no well-accepted linear mechanism for the formation of streamwise rolls and the associated streaks, nor for the selection of the observed average spanwise wavelength of 100 wall units. It is not the purpose of this paper to address these questions. Instead, we will take the streamwise rolls and streaks as given.

It is well known that such a flow cannot be a steady equilibrium solution to the Navier-Stokes equations since without streamwise variation there is no way for the structures to extract energy from the mean flow. However, the numerical work of Hamilton *et al.* (1994) shows that streamwise vortices are persistent underlying features of the flow, and that they decay on a time scale which is slow compared to the time scale of the intermittent cycle. They used a converged turbulent flow to initialize a computation with spanwise domain size too small to sustain the intermittent cycle. In this case, after one or two more cycles the flow decays away. Specifically, after the last burst of turbulence the flow relaminarizes, the three-dimensional laminar flow then decays to the x-independent streamwise rolls and streaks, and these then decay viscously to two-dimensional plane Couette flow. This decay is illustrated in Fig. 1, where the streamwise vorticity ω_x is plotted in the (y,z) plane at $x = 0$. The horizontal direction is z and the vertical is y. In these figures, the grey scale is a translation of a full color scale and is, therefore, somewhat arbitrary. The bright contours correspond to regions of negative vorticity, and the dark contours to positive vorticity. The lower left corner of the plot is the point $x = 0$, $y = -1$, $z = 0$. The flow is shown at nine equally spaced times with time increasing from the upper left to the lower right. The time scale for the entire intermittent cycle is of order 50-100. The x-dependent part of the flow decays by a factor of ten in a time of order 1-10, while the streamwise rolls decay (when $\partial/\partial x = 0$) by a factor of ten in a time of order 100.

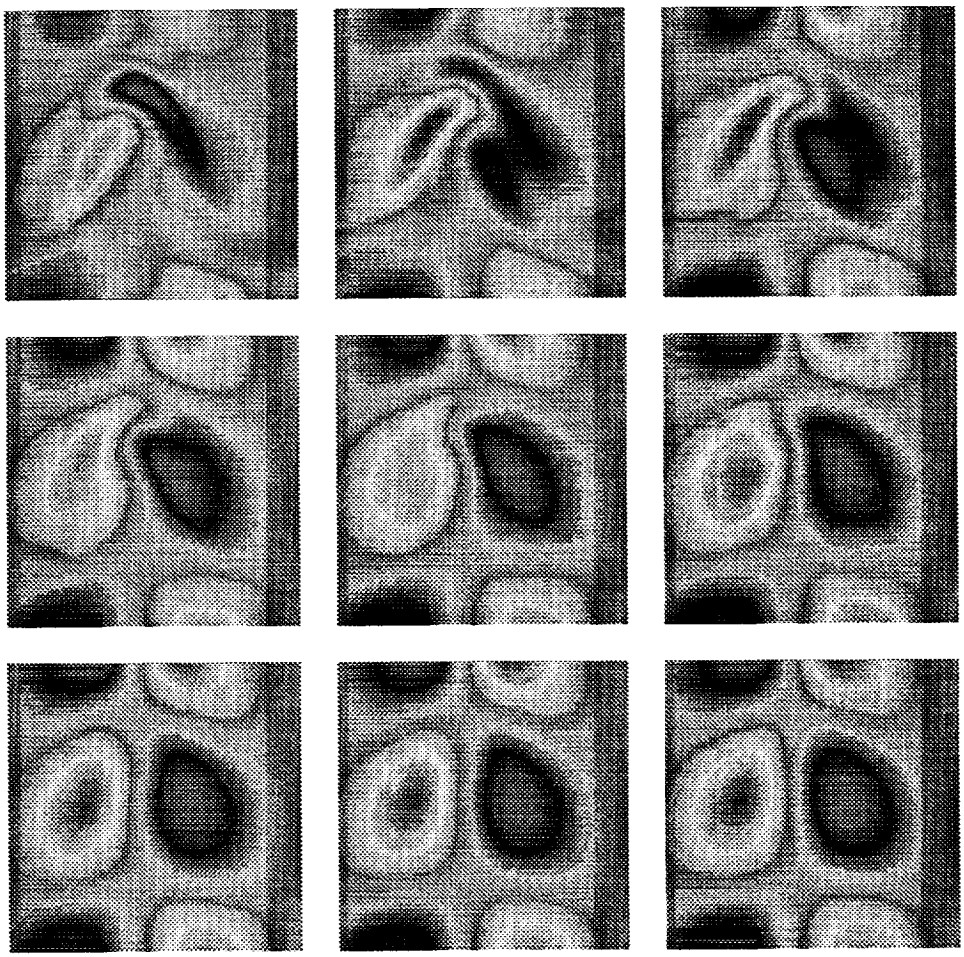

FIGURE 1. Grey-scale plots of the streamwise vorticity ω_x in the (y, z) plane at $x = 0$ at nine consecutive equally-spaced times. Time increase from left to right and top to bottom. The horizontal axis is z, and the vertical is y.

2.3 Linear stability of streamwise rolls

The separation of time scales noted above and the fact that the streamwise rolls are always the last thing to decay suggest that they are a robust quasi-equilibrium, which may be unstable to three-dimensional perturbations on a time scale fast compared to 100. A similar idea was explored by Orszag & Patera (1983) for slowly decaying Tollmein-Schlichting waves, which they found to be strongly unstable to three-dimensional modes. If there is a three-dimensional instability of the rolls, we would expect it to be the second slowest component of the flow to disappear as the turbulence dies away. The data of Hamilton *et al.* show that the configuration of the three-dimensional, decaying laminar flow is always more or less the same, as illustrated in Fig. 1. If our hypothesis is correct, then a growing linear perturbation to the rolls should, irrespective of its initial spatial configuration, end up looking

like Fig. 1 run backwards in time. This is precisely what we find in our numerical experiments.

2.4 Formal statement of the problem

Investigating the stability of a flow that is not an equilibrium is well defined if the time scale for change of the base flow is slow compared to the growth rate of the instability. Formally, we write $\mathbf{u}_{\text{rolls}} = \mathbf{u}_{\text{rolls}}(x, y, \tau)$ where $\tau \equiv \epsilon t$ defines the slow time scale for viscous decay of the vortices. From numerical experiments, we have verified that $\epsilon \sim R^{-1}$. Letting $\mathbf{u}_{\text{lin}}$ be an eigenmode of the Navier-Stokes equations linearized around $\mathbf{u}_{\text{rolls}}$, we can write (neglecting the space dependence) $\mathbf{u}_{\text{lin}} = e^{\lambda t}\mathbf{u}_{\text{lin}}(\tau)$ and consider t and τ to be independent variables. Schematically, the equation for $\mathbf{u}_{\text{lin}}$ becomes

$$(\lambda + \epsilon\partial/\partial\tau)\mathbf{u}_{\text{lin}} = \mathcal{L}\mathbf{u}_{\text{lin}} \tag{2}$$

where $\mathcal{L}$ is a linear operator depending on $\mathbf{u}_{\text{rolls}}$. By construction $\partial/\partial\tau \sim \mathcal{O}(1)$; therefore,if real$(\lambda) >> \epsilon$, we are justified in neglecting the τ dependence in Eq. (2). The simplest hypothetical instability mechanism for $\mathbf{u}_{\text{rolls}}$ is a Kelvin-Helmholtz type instability of the streak, which would have an advective time scale and therefore predict real$(\lambda) = \mathcal{O}(1)$ in our dimensionless units (Drazin & Reid, 1981). Thus, our condition for neglecting $\partial/\partial\tau$ reduces to $\epsilon \sim R^{-1} << 1$, which is well-satisfied in the cases of interest. Thus, in the discussion below we will neglect the presence of the slow time scale τ in the dynamics.

The solution $\mathbf{u}_{\text{rolls}}$ can in fact be turned into a true, steady equilibrium by adding a small forcing to the flow. Experimentally, we find that the most effective way to do this is to force the fundamental spanwise Fourier mode of v (v_{01} in Eq. (1)) to have a constant amplitude (Coughlin, 1994). Forcing v automatically forces w through the divergence equation, and v and w together produce the streak. To fix v at a value typical of the flow during the quiescent part of the cycle requires a forcing that increases the kinetic energy of the flow by less than $\sim 0.1\%$. This leads to a maximum value of v_{01} of about 0.006, and produces a streak which changes the mean profile by about 10%; hence, a very small forcing of the rolls produces a streak of fairly large amplitude. Linear instabilities of these forced rolls have the same characteristic features as those of the decaying, unforced $\mathbf{u}_{\text{rolls}}$. The forcing provides a new control parameter which can be used to look at linear stability of the rolls in a more systematic way, which will be done in future work.

3. Symmetries

The primary advantage of working with solutions having a well-defined symmetry is that the symmetry is *invariant* under nonlinear development of the flow. This can be extremely useful in understanding the origin of complicated changes in the flow pattern. These can be attributed to new bifurcations only if the symmetry changes; otherwise, no matter how much a particular visual signature of the flow may change with time, the change should (generically) be due to the generation of higher harmonics of the original linear modes. Conversely, a change in the predicted

relationships among the Fourier modes signals a qualitative change in the nature of the solution.

We have established from the numerical simulations of Couette flow that the laminar flow, started with arbitrary initial conditions, has almost exactly the symmetries described below in (Eqs. (8) and (9), and that when the flow is initialized and maintained with perfect symmetry, the dynamics is essentially unaffected. Moreover, up until the onset of turbulence, the symmetry of the initial condition doesn't change. The implication is that, beyond the onset of linear instability of $\mathbf{u}_{\text{rolls}}$, there are no other bifurcations; hence, it is the growth of the linear mode which leads to the breakdown of the laminar streak. For completeness, we present a full derivation of the relevant symmetries in this section.

3.1 Linear modes

The simplest way to deduce the allowed symmetries of the flow is to begin with the linear problem: Let $\mathbf{h}(y)e^{i(\lambda t+\alpha x+\beta z)}$+c.c. be an eigenmode of the Navier-Stokes equations linearized around the two-dimensional laminar solution U. It is then a solution to

$$\lambda h_x = (-i\alpha U + \nu\Delta)h_x - i\alpha p + \Omega h_y$$

$$\lambda h_y = (-i\alpha U + \nu\Delta)h_y - Dp$$

$$\lambda h_z = (-i\alpha U + \nu\Delta)h_z - i\beta p$$

$$0 = -i\alpha h_x + Dh_y - i\beta h_z$$

with boundary conditions $h_i(y = \pm 1) = 0$ (i labels the x, y, and z components). Here $D \equiv d/dy$ and $\Delta \equiv D^2 - \alpha^2 - \beta^2$. We define $\lambda = \sigma + i\omega$, where the growth rate σ and the phase speed ω are real.

For Couette flow, it is straightforward to show that if $(h_x, h_y, h_z)(y)$ is an eigenvector with eigenvalue λ for the parameter values (α, β), then for the same λ the following degenerate eigenvectors exist: $(-h_x, -h_y, h_z)(-y)$ for $(-\alpha, \beta)$, $(-h_x, -h_y, h_z)(y)$ for $(\alpha, -\beta)$, and $(h_x, h_y, h_z)(-y)$ for $(-\alpha, -\beta)$. When $\alpha = 0$, the eigenvectors correspond to streamwise rolls, the eigenvalue λ is real ($\omega = 0$), and the eigenfunctions satisfy $(h_x, h_y, h_z)(-y) = \pm(h_x, h_y, -h_z)(y)$. When $\alpha \neq 0$, eigenvectors with $\text{sign}(\omega/\alpha) > 0$ correspond to left-traveling waves, and their eigenfunctions h_i are not symmetric under $y \to -y$, having significant amplitude only for $y < 0$. Symmetry implies that for every left-traveling wave there is a right-traveling wave which is non-zero in $y > 0$. Since the eigenfunctions define structures, this means that these structures tend to travel with the local mean flow.

The degeneracies of linear modes for Poiseuille flow are different. In this case, for $\alpha \neq 0$ all eigenmodes have $\text{sign}(\omega/\alpha) < 0$, which again corresponds to the restriction that traveling waves go with the direction of local mean flow. For all values of α and β, the eigenfunctions satisfy $(h_x, h_y, h_z)(-y) = \pm(h_x, -h_y, h_z)(y)$. As in Couette flow, if $\alpha = 0$ the eigenvalues are real and the eigenfunctions correspond to streamwise roll solutions.

3.2 Stream-wise roll solutions

We define nonlinear streamwise rolls to be solutions resulting from the time development of the Navier-Stokes equations initialized with a linear mode with $\alpha = 0$. Note that the linear system has a higher degree of symmetry than the nonlinear, so that some of the relations found above are modified.

In the case of Couette flow, the eigenmode with maximum growth rate corresponds to a single pair of rolls in the vertical domain. In numerical experiments, this is also the nonlinear flow which emerges from arbitrary initial conditions. It has the following symmetries:

$$(u, v, w)(y, z) = (u, v, -w)(y, -z), \tag{3}$$

(reflection in z), and

$$(u, v, w)(-y, z) = (-u, -v, w)(-y, z + \pi/\beta). \tag{4}$$

The latter is the nonlinear analogue of inversion in y, which we will refer to as 'shift-and-invert' symmetry. It ensures that the streaks created by the up/down flow between the vortices at opposite walls are of equal and opposite strength. Eq. (3) implies that the rolls in a pair have opposite circulation under reflection in z.

For Poiseuille flow, the eigenmode with maximum growth rate also corresponds to a single pair of rolls in the vertical domain and leads to a nonlinear solution which satisfies (3) and

$$(u, v, w)(y, z) = (u, -v, w)(-y, z + \pi/\beta) \tag{5}$$

instead of (4). One can also obtain solutions with two roll pairs in the vertical domain; one pair of vortices is in $y \in [-1, 0]$, the other is in $y \in [0, 1]$, and there are stagnation points of the transverse flow at $(y, z) = (0, 0)$ and $(0, \pi/\beta)$. This corresponds to the eigenmode with the second largest growth rate. These solutions satisfy Eq. (3), while inversion symmetry in this case becomes

$$(u, v, w)(y, z) = (u, -v, w)(-y, z).$$

In numerical experiments, we find that the flow with two roll pairs has a higher kinetic energy than the flow with a single roll pair, and thus the former is finite-amplitude unstable to the latter (Coughlin, 1994).

3.3 Linear modes of streamwise rolls

We write down the solution for streamwise rolls as

$$\mathbf{u}_{\text{rolls}} = \sum_{m=-M/2+1}^{M/2} \mathbf{u}_m(y) e^{im\beta z} \tag{6}$$

where the origin in z is chosen such that u_m and v_m are real, and w_m is pure imaginary so that (3) is satisfied.

From Floquet theory, linear eigenmodes of the base state $\mathbf{u}_{\text{rolls}}$ will have the form

$$\mathbf{u}_{\text{lin}} = e^{i\alpha x} e^{\lambda t} \mathbf{u}'(y,z) + \text{c.c.}, \tag{7}$$

where $\mathbf{u}' = \sum_m \mathbf{u}'_m(y) e^{im\beta z}$ has the same symmetry as $\mathbf{u}_{\text{rolls}}$. Given an eigenvector $\mathbf{u}' = (u', v', w')$ with eigenvalue λ, applying symmetry operations produces new eigenfunctions with the same λ. For both Couette and Poiseuille flow, reflection in z leads to $(u', v', -w')(y, -z)$. For Couette flow, shift-and-invert symmetry produces the new vector $(-u', -v', w')(-y, z + \pi/\beta)$. If $\alpha \neq 0$ and $\text{imag}(\lambda) \neq 0$, then (as in the two-dimensional case) these linear modes correspond to left- and right-traveling waves. The left-going modes have non-zero amplitude in the region $y < 0$, while the right-going modes are of significant amplitude only in $y > 0$. For Poiseuille flow, the shift-and-invert symmetric mode is $(u', -v', w')(-y, z+\pi/\beta)$, and eigenfunctions are always even or odd in y.

3.4 Nonlinear three-dimensional flow

If the initial condition is symmetric, the time-development of the Navier-Stokes equations will, in the absence of numerical noise, preserve the symmetry. If a flow is initialized with equal amplitudes of $(u', v', w')(y, z)$ and $(u', v', -w')(y, -z)$, the nonlinear solutions will display 'shift-and-reflect' symmetry (Marcus, 1985):

$$(u, v, w)(x, y, z, t) = (u, v, -w)(x + \pi/\alpha, y, -z, t). \tag{8}$$

Note that this symmetry does not distinguish between 'sinuous' (in-phase motion of the two streaks accompanying a vortex pair) and 'varicose' (out-of-phase) modes. If the initial condition consists of equal amplitudes of $(u', v', w')(y, z)$ and $(-u', -v', w')(-y, z + \pi/\beta)$, then the three-dimensional version of shift-and-invert symmetry results. For Couette flow this is

$$(u, v, w)(x, y, z, t) = (-u, -v, w)(-x, -y, z + \pi/\beta, t). \tag{9}$$

Note that solutions with this symmetry cannot be traveling waves since there will be no translating frame in which the flow appears steady. For Poiseuille flow we have

$$(u, v, w)(x, y, z, t) = (u, -v, w)(x, -y, z + \pi/\beta, t), \tag{10}$$

instead of (9), a form which does allow traveling wave solutions.

From the Couette flow data of Hamilton *et al.* (1994) we have verified that both Eqs. (8) and (9) are satisfied approximately without being imposed on the flow. Since the code is spectral, it is convenient to express these relations in Fourier space. Using Eq. (1), shift-and-reflect symmetry becomes

$$u_{i,km}(y, t) = \gamma_i (-1)^k u_{i,k-m}(y, t).$$

Here $\gamma_i \equiv (1,1,-1)$, $u_i \equiv (u,v,w)$, and there is no sum on i. For Couette flow shift-and-invert symmetry leads to

$$u_{i,km}(-y,t) = -\gamma_i(-1)^m u_{i,-km}(y,t).$$

For a flow which is symmetric under both (8) and (9) we have

$$u_{i,km}(-y,t) = (-1)^{k+m+1}\bar{u}_{i,km}(y,t).$$

If $\mathrm{imag}(\lambda) \neq 0$, then given the form of the linear mode and the fact that the nonlinear term in the Navier-Stokes equations is quadratic, one can also predict the time dependence of individual Fourier modes (Coughlin, 1994).

4. Numerical Results

4.1 Procedures

The stability of Couette flow has been looked at in detail, and this program will be carried out for Poiseuille flow in later work. To look at the stability properties of the flow, the two procedures described below were followed:

(i) Quasi-linear initial value calculations (the same procedure was used in Hamilton *et al.*, 1994): We begin with the full solution as in Eq. (1) at some time t and from it define

$$\mathbf{u}_{\mathrm{rolls}} = \sum_{m=-M/2+1}^{M/2} \mathbf{u}_{0m}(y,t)e^{im\beta z},$$

and the perturbation

$$\mathbf{u}_{\mathrm{lin}} = e^{i\alpha x} \sum_{m=-M/2+1}^{M/2} \mathbf{u}_{1m}(y,t)e^{im\beta z} + \mathrm{c.c.}$$

The streamwise flow $\mathbf{u}_{\mathrm{rolls}}$ is frozen to its initial value, and $\mathbf{u}_{\mathrm{lin}}$ (times a constant) is added and allowed to develop in time. As long as the amplitude of $\mathbf{u}_{\mathrm{lin}}$ remains small compared to $\mathbf{u}_{\mathrm{rolls}}$, the effect of freezing the base flow is equivalent to doing a linear computation; at later times, the solution becomes unphysical.

(ii) Nonlinear initial value calculations: We define $\mathbf{u}_{\mathrm{rolls}}$ and $\mathbf{u}_{\mathrm{lin}}$ as in case (i). The flow is initialized using the combination $c_0\mathbf{u}_{\mathrm{rolls}} + c_1\mathbf{u}_{\mathrm{lin}}$, with $c_1/c_0 << 1$. The constant c_0 is used to control the strength of the rolls. While this initial condition is not a solution to the Navier-Stokes equations, after a short transient the flow settles into slowly decaying $\mathbf{u}_{\mathrm{rolls}}$ plus a linearly growing mode. The growth rate of the linear mode depends on c_0. As soon as the computation is turned on, $\mathbf{u}_{\mathrm{rolls}}$ starts to decay, and the growth rate of the instability depends very strongly on the roll amplitude, so setting $c_0 > 1$ allows the instability to develop over a longer time so that we can determine its characteristic features.

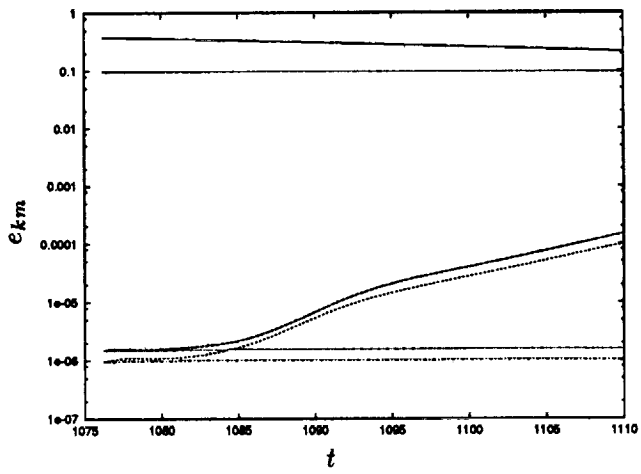

FIGURE 2. Time series of modal energies e_{km} (see text). Method (i); e_{01} ····· , e_{10} — — — , e_{11} — · — . Method (ii); e_{01} ——— , e_{10} — — — , e_{11} - - - - .

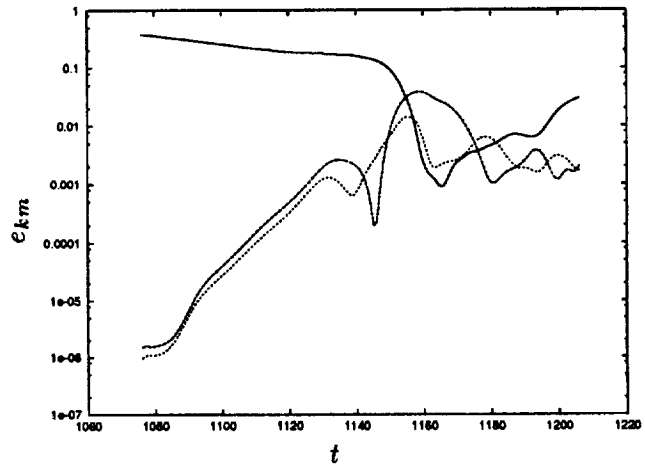

FIGURE 3. Time series of modal energies e_{km} (see text). Method (ii); e_{01} ——— , e_{10} — — — , e_{11} - - - - .

Both procedures were repeated using a different initial $\mathbf{u}_{\text{lin}} = \mathbf{u}_{11}(y,t)e^{i\alpha x}e^{i\beta z}$, where $\mathbf{u}_{11}$ is divergence-free and zero on the boundaries but otherwise arbitrary, and also with exact symmetry imposed on the initial conditions (this symmetry is maintained to order round-off error by the code). In all cases the linear mode acquires, after an initial transient, the same spatial structure and functional form in agreement with the derivation of Section 3.

4.2 Results

Method (i) was used to verify the hypothesis made above that the decaying flow configuration illustrated in Fig. 1 corresponds to a linear mode of the streamwise

rolls. The computation is initialized with the flow of Fig. 1, the decay of the rolls is halted, and the three-dimensional piece of the flow consequently stops decaying and begins to grow. It retains essentially the same spatial configuration. Recall that this configuration is also that of the fully nonlinear flow during the quiescent part of the intermittent cycle. Method (ii) was used to investigate the dependence of the growth rate σ of the three-dimensional Floquet mode on the strength of the rolls (equivalently the velocity difference across the streak), which is proportional to c_0. We find (for $R = 450$, $l_x = 1.75\pi$, and $l_z = 1.2\pi$) that $\sigma \sim c_0 - c_0^c$, with a constant of proportionality of about 0.2. Here c_0^c is the value where σ becomes negative, and depends on the initial condition. For the flow described here $c_0^c = 0.98$, so that the linear mode initially grows but starts to decay as the rolls decay. These results are consistent with the assumption that the streaks are unstable on an advective time scale. This scaling translates into a strong sensitivity of the growth rate to the strength of the rolls in the relevant regime ($c_0 \sim 1$). For example, when $c_0 \sim 1.05$, $\sigma \sim 0.01$ while for $c_0 \sim 1.6$, $\sigma \sim 0.1$. We emphasize that since the flow is in a subcritical regime, c_0 has no absolute significance, but the scaling implies that that if the energy in the streamwise flow is increased by a moderate amount, the instability growth rate can increase dramatically. We also note that apart from influencing the value of σ, the value of c_0 does not affect the linear mode; we find the same characteristic spatial pattern for all test cases.

These experiments are illustrated in Figs. 2 and 3, where we show times series of the modal energies $e_{km} = \int_{-1}^{1} |\mathbf{u}_{km}|^2 dy$ for $(k, m) = (0, 1)$ (essentially the roll amplitude), (1,0) and (1,1) (the linear modes). Note that the theoretical model predicts that modes (1,0) and (1,1) will have the same linear growth rate. In Fig. 2, these modes are plotted for two experiments using procedures (i) and (ii) with the same initial condition. In Fig. 3, the experiment using method (ii) is shown for a much longer time. We see that the (1,0) and (1,1) modes grow roughly three orders of magnitude with a nearly constant growth rate. The growth rate is not exactly constant because we do not begin the computation with the true linear eigenmode. When the $k = 1$ modes reach large enough amplitude, the flow goes over into the intermittent turbulent cycle and the time series become disordered.

4.3 Spatial structure of the linear mode

In this section we describe briefly the spatial structure of the instability of the streamwise rolls/streak. As both methods described above produce essentially the same flow, we will describe the results only for method (ii). We show in Figs. 4 and 5 visualizations of the linear instability of the rolls as it grows to finite amplitude. As in Fig. 1, we plot the streamwise vorticity ω_x using a grey scale, with dark values corresponding to positive ω_x and bright values to negative ω_x. Each frame is scaled individually so that the actual numerical value of ω_x corresponding to a particular grey level is not constant from frame to frame. Note that the change in the flow seen in these figures is due entirely to the growth of the secondary instability as it preserves the symmetry and time dependence of the flow.

Fig. 4 shows the vorticity ω_x in the (x, y) plane at nine equally spaced times with t increasing from left to right and top to bottom. The horizontal direction is

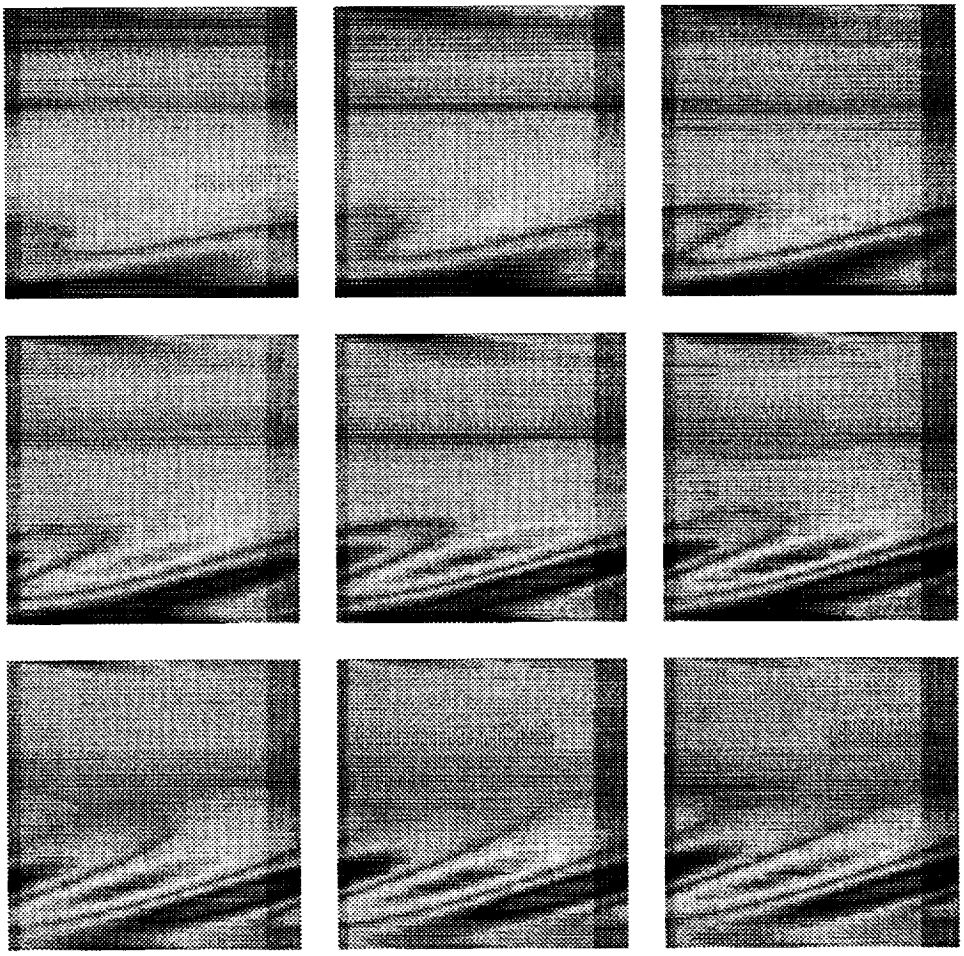

FIGURE 4. Stream-wise vorticity ω_x plotted in the (x, y) plane at $z = \pi/2\beta$, at nine consecutive equally-spaced times, for the growing three-dimensional instability. Time increase from left to right and top to bottom. The horizontal axis is x, and the vertical is y.

x and the vertical is y. This view shows a slice through the negative streamwise vortex at $z = \pi/2\beta$; the mean flow is from left to right in the lower part of the frame and from right to left in the upper part. The instability first appears as a sinusoidal deformation of the the vortex which is strongest at the cross-stream location where the vorticity ω_x changes sign. As it grows there is an interaction between the negative vorticity in the roll with the induced positive vorticity at the wall. This leads to the characteristic configuration of tilted layers of vorticity of alternating sign near the lower wall. The same pattern, inverted according to (8) and (9), appears at the upper wall at $z = 3\pi/2\beta$.

In Fig. 5 we plot ω_x in the (x, z) plane, with x the horizontal and z the vertical coordinate, for the same flow at the same times as in Fig. 4. The horizontal section

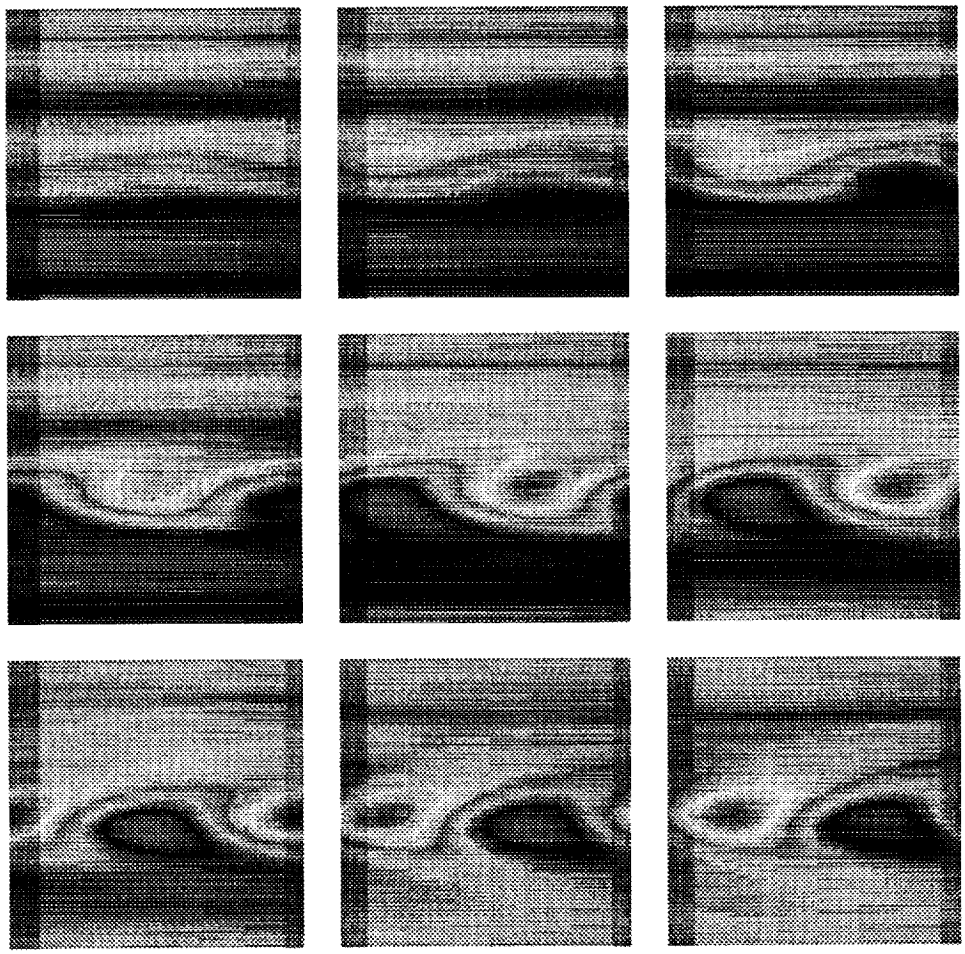

FIGURE 5. Stream-wise vorticity ω_x plotted in the (x, z) plane at $y = 0.5$ for the same flow as in Fig. 4. The horizontal axis is x, and the vertical is z.

is taken at $y = 1/2$ and passes through the upper half of the streamwise vortex pair. The streak is visualized in these plots as the grey region between the bright, negative vortex and the darker positive vortex. From these plots, it is clear that the instability begins as a waviness of the streak, which as it develops leads to a concentration of the streamwise vorticity into disc-like regions of alternating sign. These discs are tilted and layered one over the other in the (x, y) plane, as was shown in Fig. 4. The vorticity configuration seen in this plot is due primarily to the gradient $\partial w/\partial y$. It is important to note that these plots show vorticity, not vortices. Vector plots of the velocity field in the (y, z) plane, as shown for example in Hamilton *et al.* (1994), show that at all times the streamwise rolls are present; the concentration of the vorticity into the configurations seen in Figs. 1, 4, and 5 is due to a local intensification of the fluxes and gradients of the transverse velocity field. Thus, in the last row of Fig. 5, the rolls remain more or less in the same place,

but the vorticity has been concentrated into the region near the streak.

As the flow becomes more strongly nonlinear, these structures start to advect with the local mean flow, which is from left to right in Fig. 4, and in Fig. 5 from right to left. This behavior is consistent with $\mathrm{imag}(\lambda) \neq 0$ in Eq. (2), but should be verified by more detailed linear calculations. Streak break-down in this visualization corresponds to a sudden loss of the spatial regularity of the pattern and the appearance of fluctuations in the vorticity field over short time scales. Beyond this point, it is difficult to get useful information from flow visualization.

5. Conclusions

We have argued that the intermittent cycle in minimal channels consists of excursions away from a laminar base flow and that the base flow arises from linear instability of a two-dimensional flow consisting of streamwise vortices and streaks. We have shown for plane Couette flow that there is a robust, three-dimensional instability of the two-dimensional flow and that the instability can grow to large amplitude on a time scale fast relative to the decay rate of the vortices. We have given a complete description of the mathematical form of the instability and have calculated the linear mode using several (approximate) numerical techniques. We have discussed the similarities between the intermittent cycles in minimal channel flows and those occurring in the experimentally realizable Couette-Taylor system (Coughlin & Marcus, 1994). Note that these similarities suggest that the minimal channel, although it is an idealized model of the real system, does contain the relevant physics.

This study is preliminary and has raised a number of questions which we will investigate in future work. We plan to complete the analysis given above for Poiseuille flow; it would be particularly interesting to see whether the hypothesized secondary instability resembles in any way hairpin vortices. We are also interested in whether any of the mechanisms which have been proposed for the formation of streamwise vortices (for example, Butler & Farrell, 1992) are consistent with the spatial structure and stability properties of the decaying (or forced, steady) streamwise rolls found in the computations. More work also remains to be done to understand the physical nature of the instability and to what extent it can be attributed to a two-dimensional, Kelvin-Helmholz type of mechanism. Its features should also be compared in more detail to the observations of Swearingen & Blackwelder (1987) and other available experimental data.

Last but not least, there is the problem of understanding in mathematical terms the transition to turbulence. The minimal channel and Couette-Taylor simulations show that while the turbulent cycle does return intermittently to a low-dimensional dynamical state, the intervening state is almost certainly high-dimensional. The transition between them is characterized by the abrupt loss of spatial coherence of the flow, which has as yet found no adequate mathematical expression. Low dimensional models, for example as derived by Aubry *et al.* (1988) for turbulent bursts in the boundary layer of pipe flow, are inherently incapable of addressing this problem as they *a priori* eliminate most spatial degrees of freedom. The flows

discussed here isolate these fundamental issues in an elegant but not over-simplified way, and are thus deserving of further study.

REFERENCES

AUBRY, N., HOLMES, P., LUMLEY, J. L. & STONE, E. 1988 The dynamics of coherent structures in the wall region of a turbulent boundary layer. *J. Fluid Mech.* **192,** 115-173.

BUTLER, K. M. & FARRELL, B. F. 1992 Three-dimensional optimal perturbations in viscous shear flow. *Phys. Fluids A.* **4,** 1637-1650.

COUGHLIN, K. 1994 In preparation.

COUGHLIN, K. & MARCUS, P. 1994 Turbulent bursts in Couette-Taylor flow. Pre-print.

DRAZIN, P. G. & REID, W. H. 1981 *Hydrodynamic stability.*Cambridge University Press.

HAMILTON, J., KIM, J., & WALEFFE, F. 1994 Dynamics of near-wall turbulence structures. Pre-print.

HAMMIL, F., PREDTECHENSKY, A. A., SHA, E., & SWINNEY, H. L. 1994 To be published.

JIMÉNEZ, J. & MOIN, P. 1991 The minimal flow unit in near-wall turbulence. *J. Fluid Mech.* **225,** 213-240.

KIM, J., MOIN, P. & MOSER, R. 1987 Turbulence statistics in fully developed channel flow at low Reynolds number. *J. Fluid Mech.* **177,** 133-156.

ORSZAG, S. A. & PETERA, A. T. 1983 Secondary instability of wall-bounded shear flows. *J. Fluid Mech.* **128,** 347-385.

SWEARINGEN, J. D. & BLACKWELDER, R. F. 1987 The growth and breakdown of streamwise vortices in the presence of a wall. *J. Fluid Mech.* **182,** 255-290.